



# Deciphering the Protein, Modular Connections and Precision Medicine for Heart Failure With Preserved Ejection Fraction and Hypertension Based on TMT Quantitative Proteomics and Molecular Docking

## OPEN ACCESS

### Edited by:

Sanjay Kumar Banerjee,  
National Institute of Pharmaceutical  
Education and Research, Guwahati,  
India

### Reviewed by:

Vikas Kumar,  
University of Nebraska Medical  
Center, United States  
Caroline Evans,  
The University of Sheffield,  
United Kingdom

### \*Correspondence:

Yuehua Jiang  
jiang\_yuehua@hotmail.com  
Xiao Li  
lixiao617@hotmail.com

† These authors have contributed  
equally to this work

### Specialty section:

This article was submitted to  
Systems Biology Archive,  
a section of the journal  
Frontiers in Physiology

**Received:** 17 September 2020

**Accepted:** 23 September 2021

**Published:** 14 October 2021

### Citation:

Zhou G, Chen J, Wu C, Jiang P,  
Wang Y, Zhang Y, Jiang Y and Li X  
(2021) Deciphering the Protein,  
Modular Connections and Precision  
Medicine for Heart Failure With  
Preserved Ejection Fraction  
and Hypertension Based on TMT  
Quantitative Proteomics  
and Molecular Docking.  
*Front. Physiol.* 12:607089.  
doi: 10.3389/fphys.2021.607089

Guofeng Zhou<sup>1†</sup>, Jiye Chen<sup>1†</sup>, Chuanhong Wu<sup>2†</sup>, Ping Jiang<sup>1</sup>, Yongcheng Wang<sup>3</sup>,  
Yongjian Zhang<sup>1</sup>, Yuehua Jiang<sup>3\*</sup> and Xiao Li<sup>3\*</sup>

<sup>1</sup> First Clinical Medical College, Shandong University of Traditional Chinese Medicine, Jinan, China, <sup>2</sup> The Biomedical Sciences Institute of Qingdao University (Qingdao Branch of SJTU Bio-X Institutes), Qingdao University, Qingdao, China,

<sup>3</sup> Affiliated Hospital of Shandong University of Traditional Chinese Medicine, Jinan, China

**Background:** Exploring the potential biological relationships between heart failure with preserved ejection fraction (HFpEF) and concomitant diseases has been the focus of many studies for the establishment of personalized therapies. Hypertension (HTN) is the most common concomitant disease in HFpEF patients, but the functional connections between HFpEF and HTN are still not fully understood and effective treatment strategies are still lacking.

**Methods:** In this study, tandem mass tag (TMT) quantitative proteomics was used to identify disease-related proteins and construct disease-related networks. Furthermore, functional enrichment analysis of overlapping network modules was used to determine the functional similarities between HFpEF and HTN. Molecular docking and module analyses were combined to identify therapeutic targets for HFpEF and HTN.

**Results:** Seven common differentially expressed proteins (co-DEPs) and eight overlapping modules were identified in HFpEF and HTN. The common biological processes between HFpEF and HTN were mainly related to energy metabolism. Myocardial contraction, energy metabolism, apoptosis, oxidative stress, immune response, and cardiac hypertrophy were all closely associated with HFpEF and HTN. Epinephrine, sulfadimethoxine, chloroform, and prednisolone acetate were best matched with the co-DEPs by molecular docking analyses.

**Conclusion:** Myocardial contraction, energy metabolism, apoptosis, oxidative stress, immune response, and cardiac hypertrophy were the main functional connections between HFpEF and HTN. Epinephrine, sulfadimethoxine, chloroform, and prednisolone acetate could potentially be effective for the treatment of HTN and HFpEF.

**Keywords:** hypertension, heart failure with preserved ejection fraction, molecular docking, modular, therapeutic prediction

## INTRODUCTION

Heart failure with preserved ejection fraction (HFpEF), which is a complex syndrome characterized by a normal left ventricular ejection fraction and abnormal diastolic function, accounts for more than 50% of heart failure (HF) patients (Pieske et al., 2019). Current therapies for HFpEF include strategies to manage the coexisting conditions, reduce symptoms, and treat volume overload when necessary (Redfield, 2016). Although there has been much progress in HFpEF-related research, an effective strategy for HFpEF treatment has not yet been established (Gazewood and Turner, 2017). Compared with heart failure with reduced ejection fraction (HFrEF), HFpEF is heterogeneous, and drugs effective against HFrEF are not suitable for HFpEF (Graziani et al., 2018). Thus, a complete clinical phenotypic classification of HFpEF, including etiology, concomitant diseases, and risk factors, is required. Furthermore, exploring the underlying biological functions involved in the different types of HFpEF will help develop personalized therapies and precision medicines for HFpEF (Borlaug, 2020; Ge, 2020).

Patients with HFpEF that are diagnosed with hypertension (HTN) and coronary heart disease are regarded as having vascular-related HFpEF (Ge, 2020). Studies have shown that HTN is the most common complication in patients with HFpEF, but the biological relationship between HTN and HFpEF is still not fully understood (Tadic et al., 2018). In addition, studies have suggested that HTN is an additional risk factor for HFpEF (Dunlay et al., 2017). HFpEF and HTN share many common pathogeneses, such as dysfunction of cardiac autonomy, imbalance of the renin-angiotensin-aldosterone system, and excessive oxidative stress. In addition, some underlying biological mechanisms play an important role in the transition from HTN to HFpEF. For example, hypertension leads to diastolic dysfunction and concentric remodeled left ventricular decompensation, resulting in HFpEF (Drazner, 2011; Heinzel et al., 2015; Messerli et al., 2017; Nwabuo and Vasan, 2020). In addition, HTN also activates chronic inflammation and increases collagen deposition, further exacerbating left ventricular dysfunction (Paulus and Tschöpe, 2013). Studies have reported that myocardial contractile dysfunction, right ventricular dysfunction, arterial stiffness, ventricular-arterial coupling, and microvascular dysfunction could increase the risk of HFpEF in patients with HTN (Hicklin et al., 2020). However, in clinical trials, drugs such as angiotensin-converting enzyme inhibitors, angiotensin II receptor blockers, diuretics, and beta-blockers, which showed beneficial effects against common pathogeneses of HFpEF and HTN, did not produce significant positive effects in patients with HFpEF (Kjeldsen et al., 2020). Therefore, further research is needed to explore the potential biological relationships between HFpEF and HTN.

Disease network construction provides a solution to explore the relationships between diseases (Le and Pham, 2017), where modules of disease-related networks are responsible for various features of the diseases. Functional enrichment analysis of the overlapping modules reflects the functional links among related diseases (Dean et al., 2017). For example, using this method, a previous study showed that the negative

regulation of transcription from RNA polymerase II promoter RNA and the negative regulation of apoptotic processes are overlapping biological functions among type-2 diabetes mellitus, prostate cancer, and chronic myeloid leukemia (Liu et al., 2019). Furthermore, another study showed that atherosclerosis, cholesterol homeostasis, plasma lipoprotein particle remodeling, and oxidative stress responses are common risk factors for stroke and coronary heart disease (Zhang et al., 2014).

The Dahl salt-sensitive (DS) rat model has been implemented for the study of HFpEF (Cho et al., 2017). Toward that, DS rats diagnosed with HTN or HFpEF were analyzed using proteomics. Cytoscape software and STRING platforms were used to construct a disease network. Modules of the disease network were divided using Molecular Complex Detection (MCODE). Gene Ontology (GO) enrichment analysis was performed to identify the significant functions and pathways of overlapping modules found in the Database for Annotation, Visualization, and Integrated Discovery (DAVID). Molecular docking and module analyses were combined to contribute to the development of personalized therapies and precision medicines for HFpEF and HTN treatment. A flowchart of the research design is shown in **Figure 1**.

## MATERIALS AND METHODS

### Animals and Experimental Protocols

Specific pathogen-free 6-week-old male DS rats (weight: 160–180 g; Certificate No. 2016-0006) were obtained from the Charles River Animal Laboratory (Beijing, China). Rats were housed in groups of six rats per cage under controlled conditions (12 h dark/light cycle, temperature: 20–24°C, relative humidity: 40–60%, dB ≤ 60) and with free access to water and food. After a week of adaptation, the rats were randomly divided into the following three groups: the HTN group (8% NaCl chow for 7 weeks,  $n = 6$ ), the HFpEF group (8% NaCl chow for 11 weeks,  $n = 6$ ), and the control group (0.3% NaCl chow for 7 or 11 weeks,  $n = 12$ ). All experiments were reviewed by the Animal Ethics Committee of the Shandong University of Traditional Chinese Medicine (Ethics No. SDUTCM2018071501).

### Tissue Collection

The rats in the HTN and HFpEF groups were euthanized after 7 and 11 weeks of the high-salt diet (HSD), respectively, and the rats in the control group were randomly sacrificed after 7 or 11 weeks of the control diet. Pentobarbital (20 mg/kg, i.p.) was used for anesthesia in rats, and the left ventricle (LV) was collected from each rat and stored at  $-80^{\circ}\text{C}$ .

### Tandem Mass Tag-Labeled Quantitative Proteomics

Twelve LV samples [HTN group  $n = 3$ , HFpEF group  $n = 3$ , control group (euthanized at 7 weeks)  $n = 3$ , control group (euthanized at 11 weeks)  $n = 3$ ] were collected for TMT quantitative proteomics. Previous studies reported that data with three samples in each group could reliably be statistically

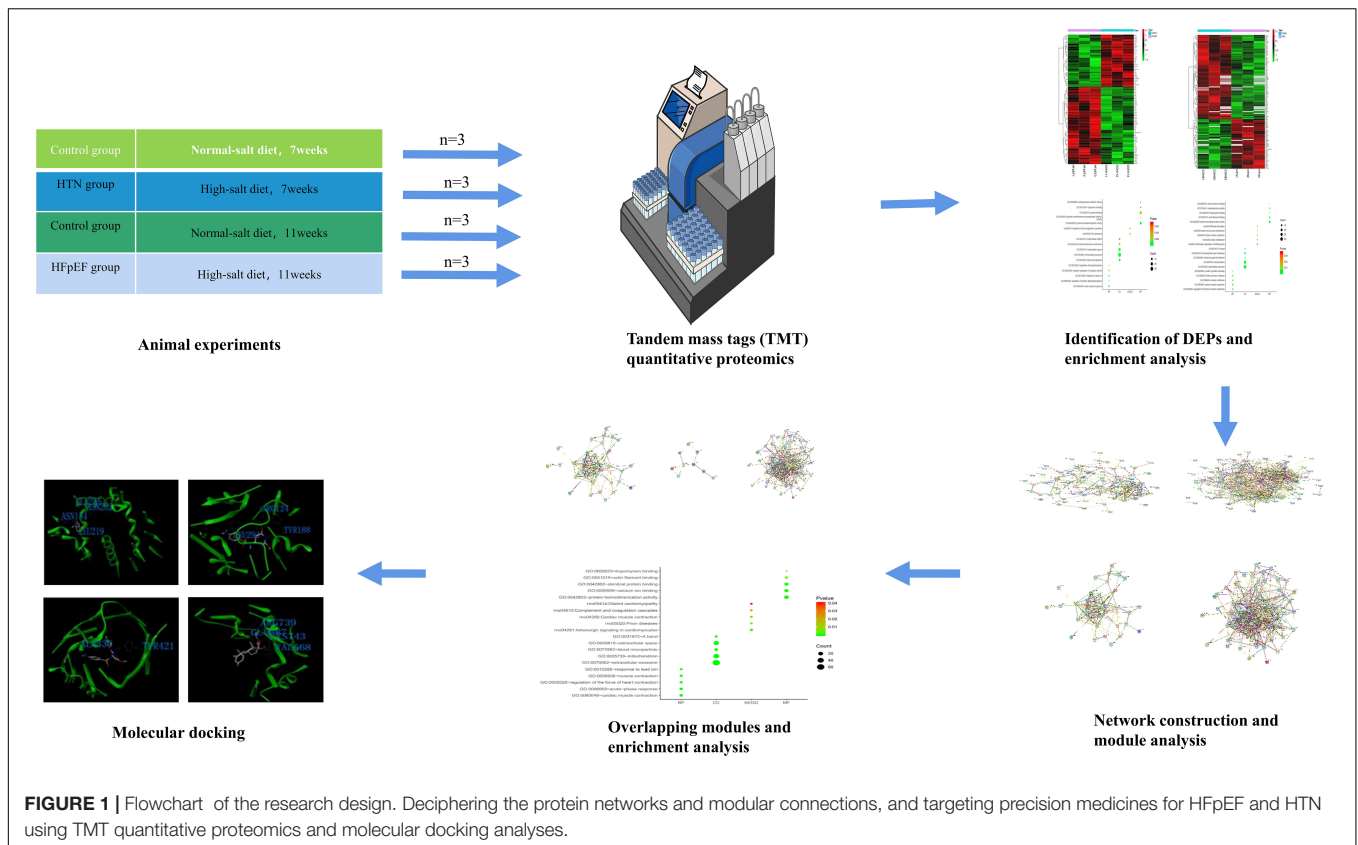


**FIGURE 1** | Flowchart of the research design. Deciphering the protein networks and modular connections, and targeting precision medicines for HFpEF and HTN using TMT quantitative proteomics and molecular docking analyses.

analyzed (Maitiabola et al., 2020; Yan et al., 2020). The tissue was removed from the refrigerator at  $-80^{\circ}\text{C}$ , ground into powder, and quickly transferred to a centrifuge tube pre-cooled with liquid nitrogen. PASP protein lysate (100 mM ammonium bicarbonate, 8 M urea, pH 8) was added to the liquid nitrogen, shaken, mixed, and ultrasonicated in an ice water bath for 5 min, followed by centrifugation at 12,000 rpm for 15 min at  $4^{\circ}\text{C}$ . Then, the supernatant was collected, 10 nM dithiothreitol was added, and the mixture was incubated at  $56^{\circ}\text{C}$  for 1 h. Then, iodoacetamide was added and the reaction was allowed to proceed for 1 h in the absence of light. Next, four volumes of pre-cooled acetone were used for precipitation, followed by centrifugation at 12,000 rpm for 15 min at  $4^{\circ}\text{C}$ , after which the precipitate was collected. The precipitate was resuspended and washed with one milliliter of  $-20^{\circ}\text{C}$  pre-cooled acetone, followed by a second centrifugation at 12,000 rpm for 15 min at  $4^{\circ}\text{C}$ . Then, the precipitate was collected and air dried, and an appropriate amount of protein dissolving solution (8 M urea, 100 mM TEAB, pH 8.5) was used to dissolve the protein precipitate.

The Bradford protein quantification kit (Beyotime, China) was used to determine the protein concentration. DB protein dissolving solution (8 M urea, 100 mM TEAB, pH 8.5) was added to the protein sample to a volume of 100  $\mu\text{L}$ , trypsin and 100 mM buffer were added, and mixing and digestion were performed at  $37^{\circ}\text{C}$  for 4 h. Then, pancreatin and  $\text{CaCl}_2$  were used for digestion overnight. Formic acid was used to adjust the pH to less than

3, mixing was done at room temperature, and centrifugation was performed at 12,000 rpm for 5 min. The supernatant was then slowly passed through the C18 desalting column, and the cleaning solution (0.1% formic acid, 3% acetonitrile) was used for washing three times. In addition, an appropriate amount of eluent (0.1% formic acid, 70% acetonitrile) was added, and the filtrate was collected and lyophilized. One hundred microliters of 0.1 M TEAB buffer was used for reconstitution, and 41  $\mu\text{L}$  of TMT labeling reagent was dissolved in acetonitrile. The mixture was mixed at room temperature for 2 h, and 8% ammonia was added to stop the reaction. An equal volume of the labeled sample was used for mixing and freeze-drying after desalting.

Mobile phase A solution (2% acetonitrile, 98% water, pH 10) and mobile phase B solution (98% acetonitrile, 2% water) were prepared. The freeze-dried powder was dissolved in solution A and centrifuged at 12,000 rpm for 10 min at room temperature. An L-3000 HPLC system and a water VEHC 18 (4.6 mm  $\times$  250 mm, 5  $\mu\text{m}$ ) were used for this study, and the column temperature was set to  $45^{\circ}\text{C}$ . Details of the elution gradient are shown in **Table 1**. One tube was collected every minute, divided into 10 fractions, freeze-dried, and dissolved in 0.1% formic acid.

Mobile phase A solution (100% water, 0.1% formic acid) and phase B solution (80% acetonitrile, 0.1% formic acid) were prepared. One microgram of the supernatant from each fraction was used for the test. The UHPLC system was upgraded

**TABLE 1** | The elution gradient table of peptide fraction separation liquid chromatography.

Time (min)	Flow rate (mL/min)	Mobile phase A (%)	Mobile phase B (%)
0	1	97	3
10	1	95	5
30	1	80	20
48	1	60	40
50	1	50	50
53	1	30	70
54	1	0	100

with the EASY-nLC 1200 system. We prepared both the pre-column (4.5 cm × 75 μm, 3 μm) and the analytical column (15 cm × 150 μm, 1.9 μm). The elution conditions for liquid chromatography are shown in **Table 2**. A Q Exactive series mass spectrometer was used for this study, the ion source was the Nanospray Flex, the ion spray voltage was 2.3 kV, the temperature of the ion transfer tube was 320°C, and the data-dependent acquisition mode was used. The full scan range of the mass spectrum was 350–1,500 m/z. The resolution of the primary mass spectrometry was set to 60,000 (200 m/z), the maximum capacity of the C-trap was  $3 \times 10^6$ , and the maximum injection time of the C-trap was 20 ms. The top 40 precursor ions were selected for the full scan, and the higher-energy collision dissociation (HCD) method was used for the fragment, which contributed to the secondary mass spectrometry detection. The isolation window of MS2 spectrum is 2 m/z. HCD spectrum ranged from 120 to m/z (precursor ion) × z (charge number) + 100 m/z. The resolution was 45,000 (200 m/z), the maximum capacity of the C-trap was  $5 \times 10^4$ , the maximum injection time of the C-trap was 86 ms, the threshold intensity was  $1.2 \times 10^5$ , and the dynamic exclusion range was 20 s.

MS/MS raw files were processed using the MASCOT engine (Matrix Science, London, United Kingdom; version 2.6) embedded into Proteome Discoverer software, and searched against the UniProt database, including Uniprot\_RattusNorvegicus\_36080\_20180123 sequences<sup>1</sup>. The search parameters included trypsin as the enzyme used to generate peptides with a maximum of two missed cleavages permitted. A precursor mass tolerance of 10 ppm was specified along with a 0.05 Da tolerance for MS2 fragments. Except for the TMT labels, carbamidomethyl (C) was set as a fixed modification. The variable modifications were oxidation (M) and acetyl (protein N-term). A peptide and protein false discovery rate of 1% was enforced using a reverse database search strategy. The quantitative values of proteins obtained from two pairs of samples were examined using the *t*-test, and the *p*-values were calculated. Fold change >1.1, fold change <0.91, and *P*-value < 0.05, were considered to filter differentially expressed proteins (DEPs). Proteomic data is provided as **Supplementary Material**.

<sup>1</sup><http://www.uniprot.org>

**TABLE 2** | Elution gradient table of liquid chromatography.

Time (min)	Flow rate (nL/min)	Mobile phase A (%)	Mobile phase B (%)
0	600	94	6
2	600	85	15
78.5	600	60	40
80.5	600	50	50
81.5	600	45	55
90	600	0	100

## Constructing the Protein-Protein Interaction Networks for Heart Failure With Preserved Ejection Fraction and Hypertension

The STRING database (version 10.5)<sup>2</sup> was used to predict protein interactions and functional associations. The PPI networks of HFpEF- and HTN-DEPs were obtained under controlled parameters (interaction score > 0.4). PPI networks were analyzed using Cytoscape (version 3.6.1)<sup>3</sup>.

## Functional Enrichment Analysis

HFpEF- and HTN-DEPs were submitted to the Database for annotation, visualization, and integrated discovery for functional enrichment, including GO and Kyoto Encyclopedia of Genes and Genomes (KEGG) pathway enrichment analyses (version 6.8)<sup>4</sup>. The *P*-value was set at <0.05 for GO and KEGG pathway enrichment, as is standard in the field (Yuan et al., 2016; Liu et al., 2019).

## Division and Identification of Network Modules

Disease-related networks were analyzed using Cytoscape (version 3.6.1)<sup>5</sup>. Furthermore, the modules were divided by Molecular Complex Detection (MCODE, version 1.3.2)<sup>6</sup>. The modules were obtained under controlled parameters (degree cutoff = 2, node score cutoff = 0.1, core threshold *K* = 2, flux density cutoff = 0.1, *K*-core 2, max. depth = 100). The parameters for Cytoscape were set as default, as recommended by previous studies (Yuan et al., 2016; Liu et al., 2019).

## Identification of Modern Medicine Symptoms Related to Common Differentially Expressed Proteins and Links to Cardiovascular Diseases

The association between the co-DEPs and cardiovascular diseases was analyzed using the Comparative Toxicogenomics Database (CTD)<sup>7</sup>, which integrates the relationships between gene

<sup>2</sup><http://string-db.org/>

<sup>3</sup><https://cytoscape.org/>

<sup>4</sup><https://david.ncicrf.gov/>

<sup>5</sup><https://www.cytoscape.org/>

<sup>6</sup><https://baderlab.org/Software/MCODE>

<sup>7</sup><http://ctdbase.org/>

products, diseases, chemicals, and environments. Furthermore, related MM symptoms of the co-DEPs were observed in SymMap<sup>8</sup> and in previous publications.

## Drug Discovery and Molecular Docking

Small-molecule compounds related to the co-DEPs were observed from the DrugBank<sup>9</sup>, through the target search. Molecular docking analysis is a common strategy for drug discovery. The structures of the co-DEPs were downloaded from the Protein Data Bank (PDB)<sup>10</sup>, and the PDB IDs of the proteins are shown in **Table 3**. The structures of the drugs were obtained from PubChem<sup>11</sup>, and the CIDs are shown in **Table 4**. Eutectic ligands and water molecules were removed, and residue repair, side chain fixation, and hydrogenation were used for protein preparation. The Surflex-Dock module of SYBYL 2.1 was used for molecular docking. Furthermore, AMBR7 was used for energy optimization, and the active pockets were obtained in automatic mode. The parameters for SYBYL 2.1 were set as default, as recommended by previous studies (Tan et al., 2020). The molecular docking scores reflected the binding effects between the small-molecule compounds and the co-DEPs, and the highest scoring small molecules were considered as potential drugs.

## RESULTS

### Identification of Differentially Expressed Proteins

A total of 83 DEPs, including 52 upregulated proteins, were obtained by comparing the HFpEF group with the control group sacrificed at 11 weeks (**Figure 2A**). A total of 132 DEPs, including 85 upregulated proteins, were identified by comparing the HTN group with the control group sacrificed at 7 weeks (**Figure 2B**). Among the HFpEF-DEPs and HTN-DEPs, there were 7 co-DEPs, including haptoglobin (Hp), coenzyme Q9 (COQ9), serotransferrin (Tf), major prion protein (Prnp), acetyl-CoA acetyltransferase, mitochondrial (Acat1), translocase of inner mitochondrial membrane 44 (Timm44), and ATP-binding cassette sub-family B member 6 (Abcb6; **Figure 2C**). Furthermore, the CTD database showed links

<sup>8</sup><https://www.symmap.org/>

<sup>9</sup><https://www.drugbank.ca/>

<sup>10</sup><http://www.rcsb.org/>

<sup>11</sup><https://pubchem.ncbi.nlm.nih.gov/>

**TABLE 3** | PDB ID of protein.

Protein	PDB ID
Hp	4XOIL
COQ9	6awl
Tf	1ryo
Prnp	2ol9
Acta1	2lb8
Timm44	2cw9
Abcb6	3nh6

**TABLE 4** | CIDs of molecule compounds.

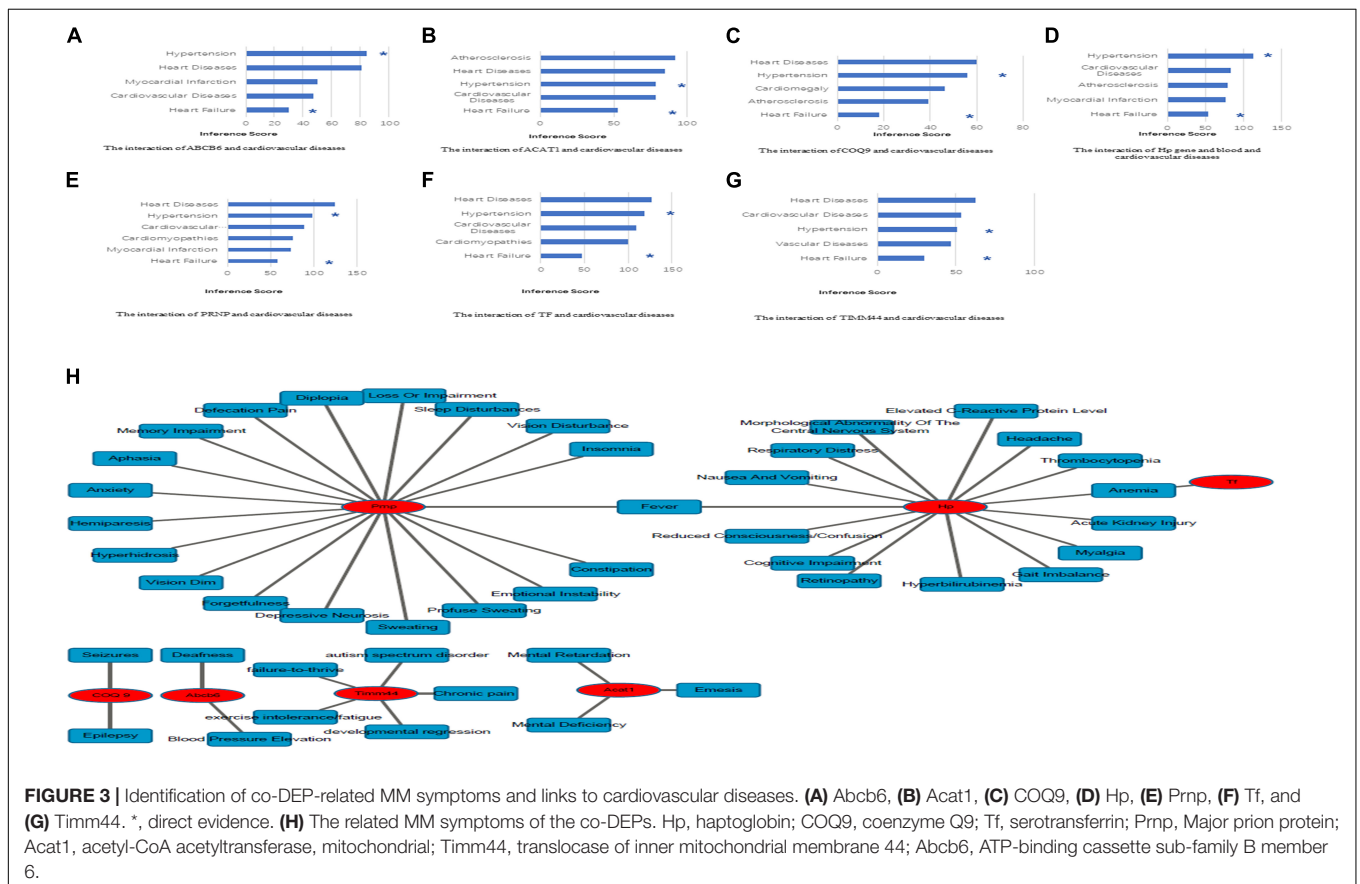
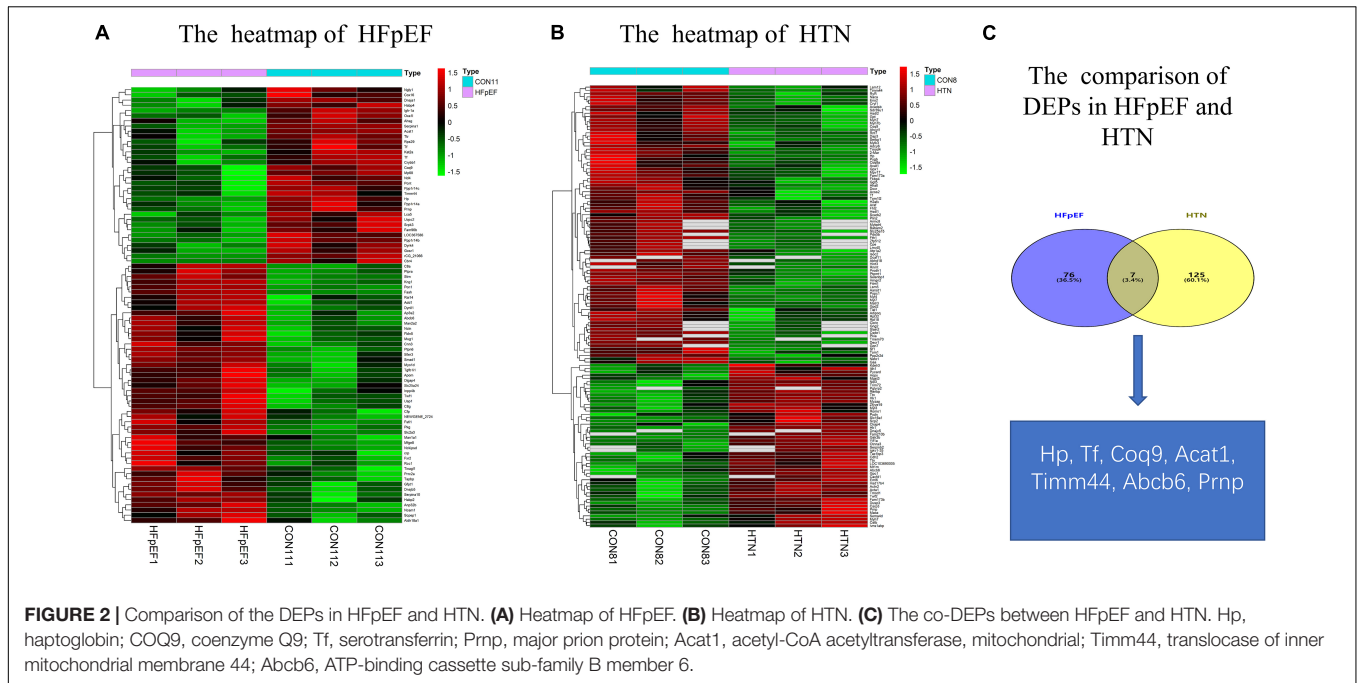
Molecule	PubChem ID
Prednisolone acetate	5834
Bismuth subsalicylate	16682734
Phenoxyethylpenicillin	6869
Polyethylene glycol	40786
Prednisolone	5755
Chloroform	6212
Salicylic acid	338
Epinephrine	5816
Triptorelin	25074470
Benzylpenicillin	5904
Propofol	4743
Sulfadimethoxine	5323

between the co-DEPs and various cardiovascular diseases (**Figures 3A–G**). Finally, the related MM symptoms of the co-DEPs were determined using SymMap<sup>12</sup> and previous publications (**Figure 3H**).

### Functional Enrichment Analysis

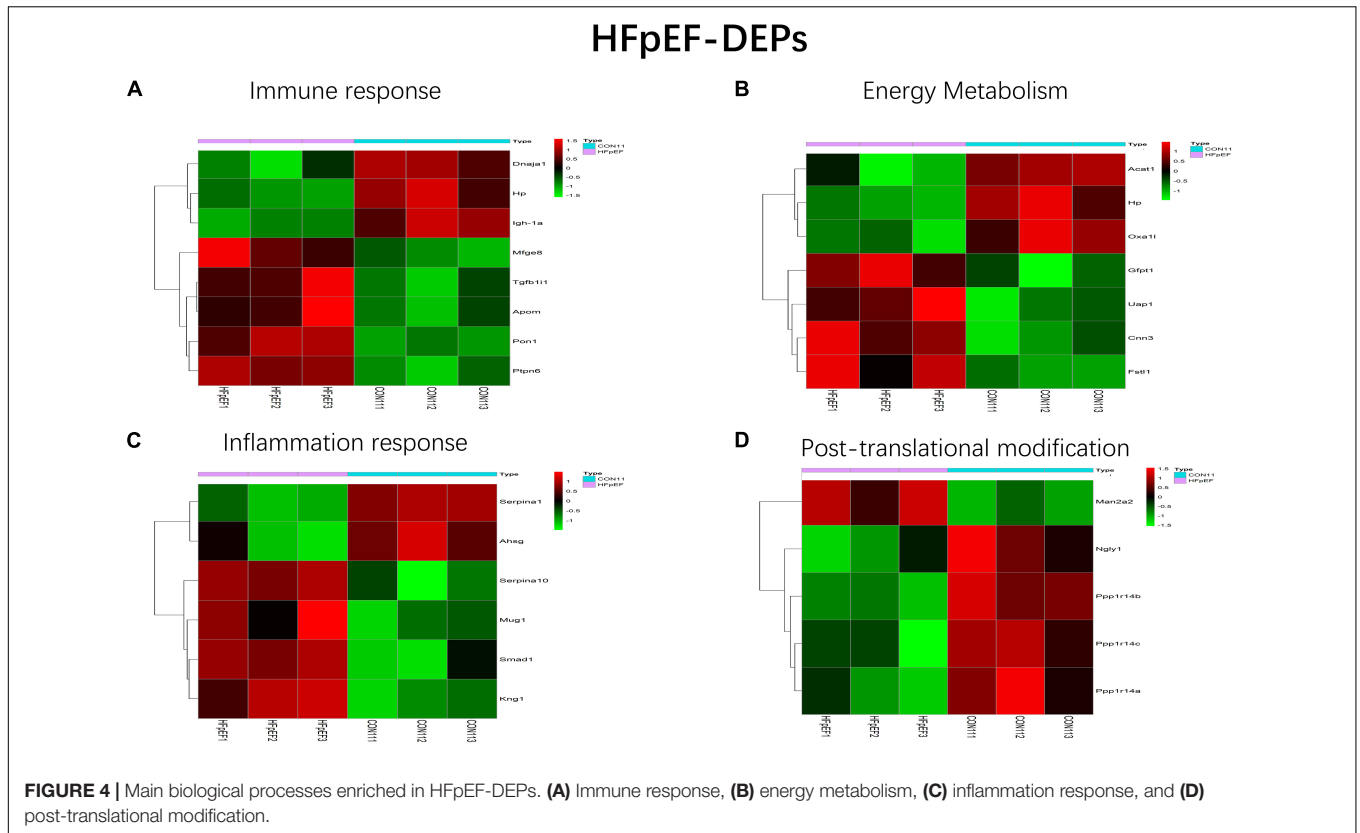
All HFpEF- and HTN-DEPs were submitted to DAVID for GO and KEGG functional enrichment analyses. The DEPs of HFpEF were mainly involved in immune response, energy metabolism, inflammation response, and post-translational modification (**Figure 4**). For example, DnaJ heat shock protein family (Hsp40) member A1 (Dnaj1), Hp, immunoglobulin heavy chain 6 (Igh-1a), milk fat globule EGF and factor V/VIII domain containing (Mfge8), transforming growth factor beta 1 induced transcript 1 (Tgfb1i1), apolipoprotein M (Apom), paraoxonase 1 (Pon1), protein tyrosine phosphatase, and non-receptor type 6 (Ptpn6) were closely related to immune response; acetyl-CoA acetyltransferase, mitochondrial (Acta1), Hp, mitochondrial inner membrane protein (Oxa11), glutamine fructose-6-phosphate transaminase 1 (Gfpt1), UDP-N-acetylglucosamine pyrophosphorylase 1 (Uap1), calponin 3 (Cnn3), and follistatin-like 1 (Fstl1) were involved in energy metabolism; serpin family A member 1 (Serpina1), alpha-2-HS-glycoprotein (Ahsg), serpin family A member 10 (Serpina10), murinoglobulin 1 (Mug1), SMAD family member 1 (Smad1), and kininogen 1 (Kng1) were connected with inflammation response; mannosidase, alpha, class 2A, member 2 (Man2a2), N-glycanase 1 (Ngly1), protein phosphatase 1, regulatory (inhibitor) subunit 14B (Ppp1r14b), protein phosphatase 1, regulatory (inhibitor) subunit 14C (Ppp1r14c), protein phosphatase 1, and regulatory (inhibitor) subunit 14A (Ppp1r14a) were involved in post-translational modification. For HTN, myocardial contraction, energy metabolism, apoptosis, and oxidative stress were the main biological functions (**Figure 5**). Carcass protein in high growth mice 3 (Carp3), myosin light chain 3 (Myl3), titin (Ttn), tropomodulin (Tmod1), hydroxysteroid (17-beta) dehydrogenase 4 (Hsd17b4), actinin alpha 2 (Actn2), Acta1,

<sup>12</sup>[https://www.symmap.org](https://www.symmap.org/)



myosin, light chain 4 (Myl4), Tf, alpha glucosidase (Gaa), perilipin 2 (Plin2), ATPase Na<sup>+</sup>/K<sup>+</sup> transporting subunit alpha 2 (Atp1a2), enolase 2 (Eno2), myosin heavy chain 7 (Myh7),

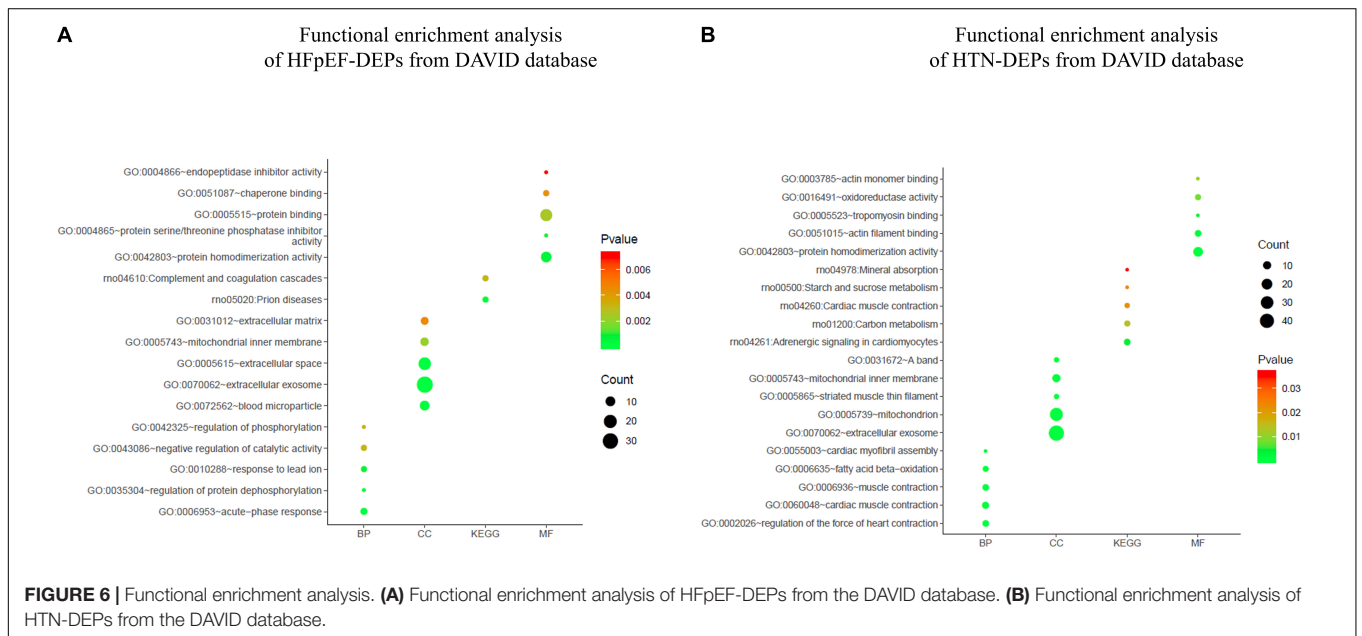
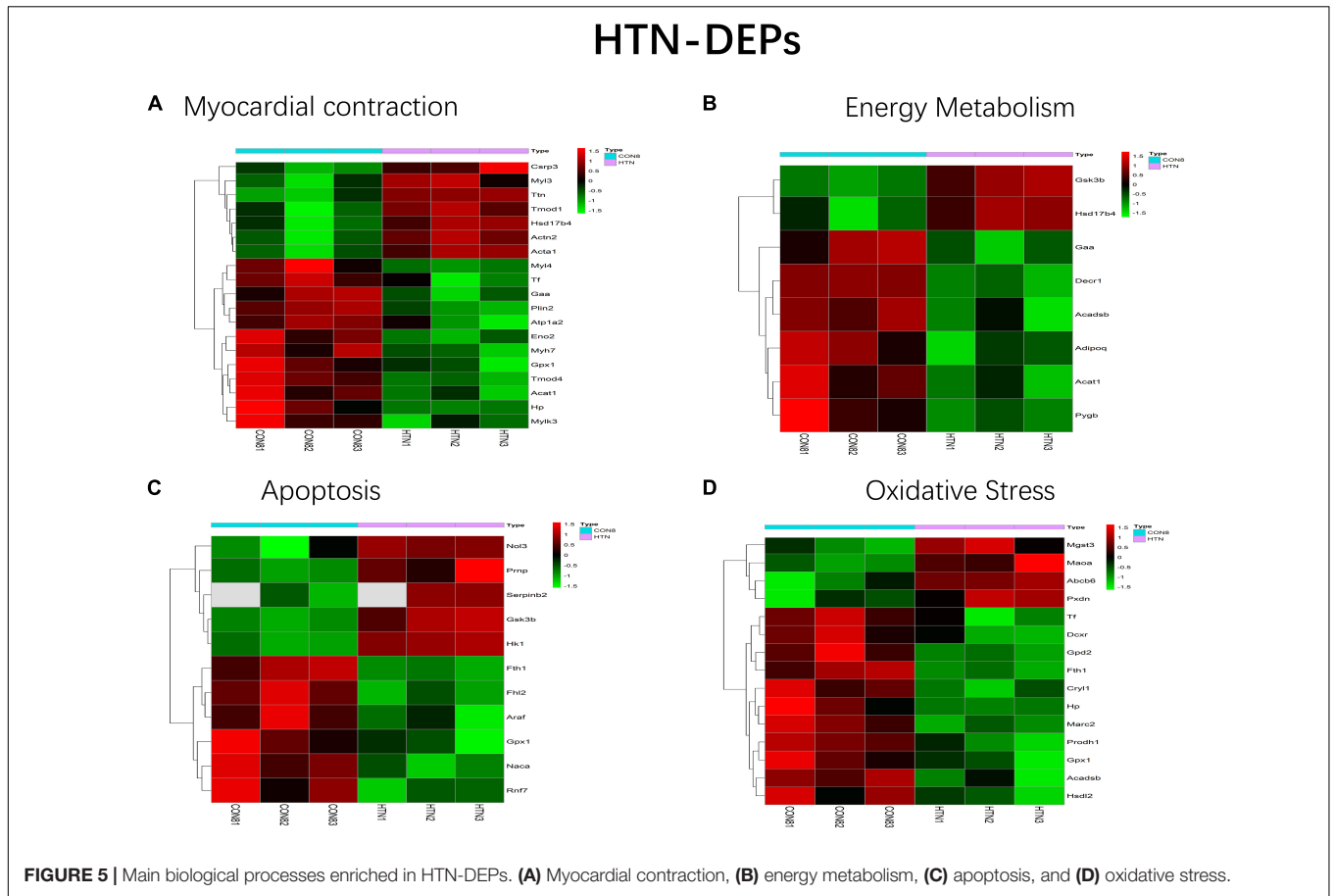
glutathione peroxidase 1 (Gpx1), tropomodulin 4 (Tmod4), Acta1, Hp, and myosin light chain kinase 3 (Mylk3) were closely related to myocardial contraction; glycogen synthase kinase

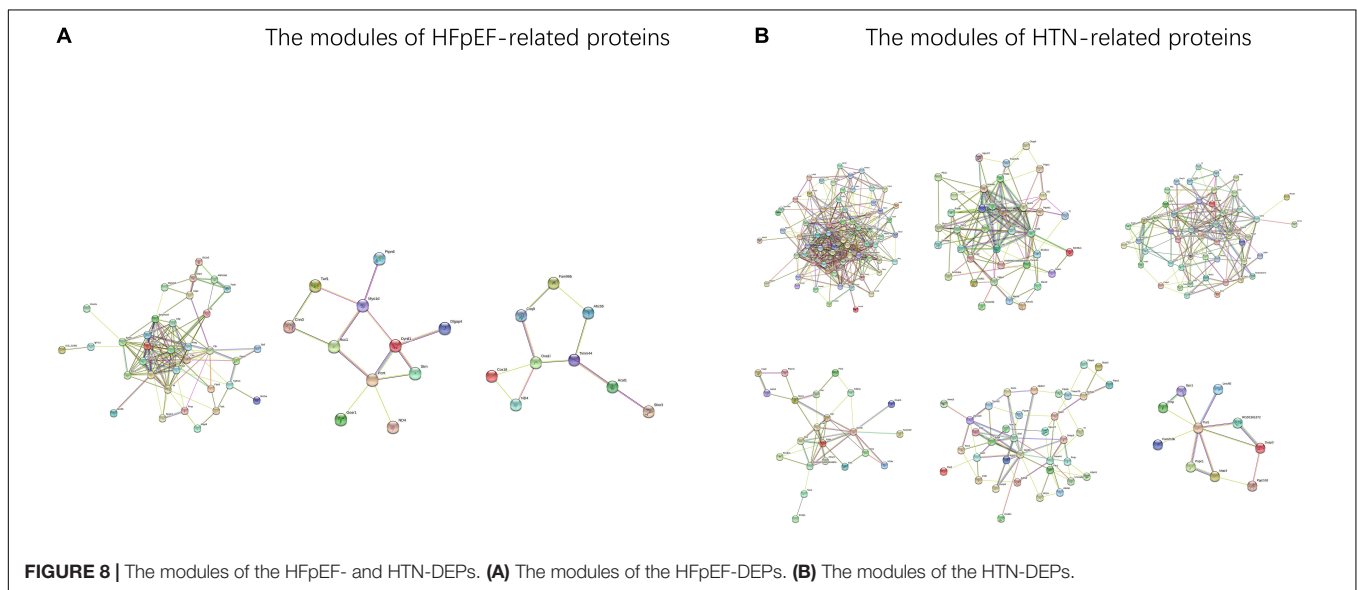
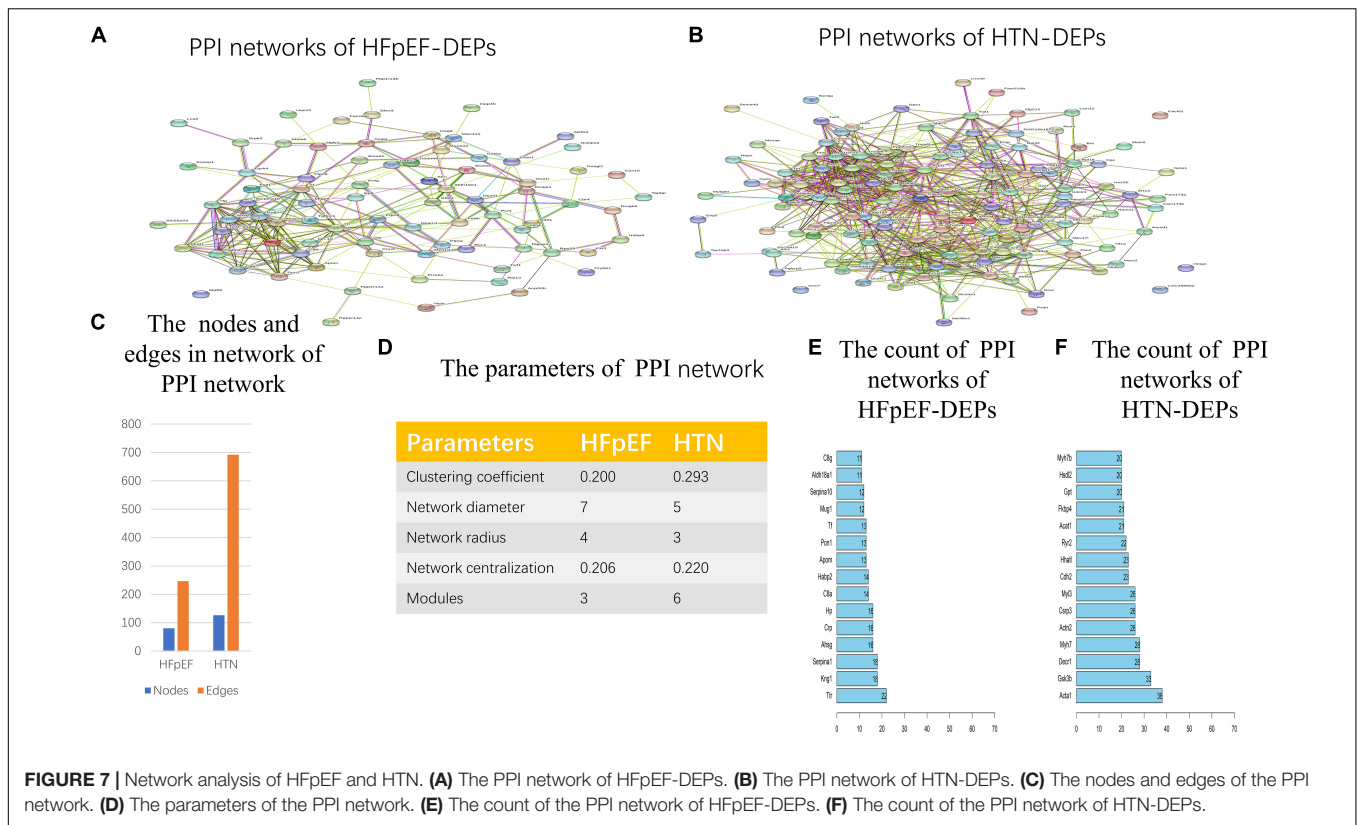


3 beta (Gsk3b), hydroxysteroid (17-beta) dehydrogenase 4 (Hsd17b4), alpha glucosidase (Gaa), 2,4-dienoyl-CoA reductase 1 (Decr1), acyl-CoA dehydrogenase, short/branched chain (Acadsb), adiponectin C1Q and collagen domain containing (Adipoq), Acta1, and glycogen phosphorylase B (Pygb) were involved in energy metabolism; nucleolar protein 3 (Nol3), prion protein (Prnp), serpin family B member 2 (Serpinb2), glycogen synthase kinase 3 beta (Gsk3b), hexokinase 1 (Hk1), ferritin heavy chain 1 (Fth1), four and a half LIM domains 2 (Fhl2), A-Raf proto-oncogene, serine/threonine kinase (Araf), glutathione peroxidase 1 (Gpx1), nascent polypeptide associated complex subunit alpha (Naca), and ring finger protein 7 (Rnf7) were connected with apoptosis.

The top five biological processes among HFpEF-DEPs were acute-phase response (count 5, *P*-Value 2.15E-05), regulation of protein dephosphorylation (count 3, *P*-Value 2.75E-04), response to lead ion (count 4, *P*-Value 6.39E-04), negative regulation of catalytic activity (count 4, *P*-Value 0.003203462), and regulation of phosphorylation (count 3, *P*-Value 0.003348677). Blood microparticles (count 10, *P*-Value 1.80E-09), extracellular exosome (count 33, *P*-Value 1.01E-08), extracellular space (count 18, *P*-Value 3.18E-05), mitochondrial inner membrane (count 7, *P*-Value 0.002195356), and extracellular matrix (count 6, *P*-Value 0.00460952) related cell compositions were significantly enriched. Furthermore, the main enriched molecular functions were protein homodimerization activity (count 12, *P*-Value 5.67E-04), protein serine/threonine phosphatase inhibitor activity (count 3, *P*-Value 9.62E-04), protein binding (count

16, *P*-Value 0.002503286), chaperone binding (count 4, *P*-Value 0.004337384), and endopeptidase inhibitor activity (count 3, *P*-Value 0.007219962). The enriched KEGG pathways were prion diseases (count 4, *P*-Value 3.21E-04) and the complement and coagulation cascades (count 4, *P*-Value 0.003144821) (**Figure 6A**). With respect to HTN-DEPs, the most enriched biological processes were the regulation of heart contraction force (count 6, *P*-Value 2.73E-07), cardiac muscle contraction (count 7, *P*-Value 5.96E-07), muscle contraction (count 6, *P*-Value 1.50E-05), fatty acid beta-oxidation (count 5, *P*-Value 1.95E-04), and cardiac myofibril assembly (count 3, *P*-Value 0.002067005). The main components were extracellular exosome (count 48, *P*-Value 3.12E-11), mitochondrion (count 32, *P*-Value 3.12E-08), striated muscle thin filament (count 4, *P*-Value 3.24E-05), mitochondrial inner membrane (count 10, *P*-Value 2.30E-04), and a band (count 4, *P*-Value 4.49E-04). The molecular functions of HTN-DEPs were mainly enriched in protein homodimerization activity (count 15, *P*-Value 4.74E-04), actin filament binding (count 6, *P*-Value 0.001790743), tropomyosin binding (count 3, *P*-Value 0.003348376), oxidoreductase activity (count 5, *P*-Value 0.00825633), and actin monomer binding (count 3, *P*-Value 0.010556462). The enriched KEGG pathways were adrenergic signaling in cardiomyocytes (count 6, *P*-Value 0.004149388), carbon metabolism (count 5, *P*-Value 0.014082125), cardiac muscle contraction (count 4, *P*-Value 0.022270779), starch and sucrose metabolism (count 3, *P*-Value 0.023739862), and mineral absorption (count 3, *P*-Value 0.03637201) (**Figure 6B**).





### Protein-Protein Interaction Network Analysis and Modularity Analysis

In total, from the PPI network of HFpEF-DEPs (**Figure 7A**) and that of the HTN-DEPs (**Figure 7B**), 80 nodes and 246 edges, and 126 nodes and 692 edges were identified, respectively (**Figure 7C**). The parameters of the PPI network of the HFpEF- and HTN-DEPs are shown in **Figure 7D**. Furthermore, transthyretin (Ttr; degree = 22), kininogen-1

(Kng1; degree = 18), alpha-1-antiproteinase (Serpina1; degree = 18), alpha-2-HS-glycoprotein (Ahsg; degree = 16), and pentaxin (Crp; degree = 16) were identified as hub proteins in the HFpEF-DEP PPI network (**Figure 7E**). Acetyl-CoA acetyltransferase, mitochondrial (Acta1; degree = 38), glycogen synthase kinase 3 beta (Gsk3b; degree = 33), 2,4-dienoyl-CoA reductase 1 (Decr1; degree = 28), myosin heavy chain 7 (Myh7; degree = 28), and actinin alpha 2 (Actn2;



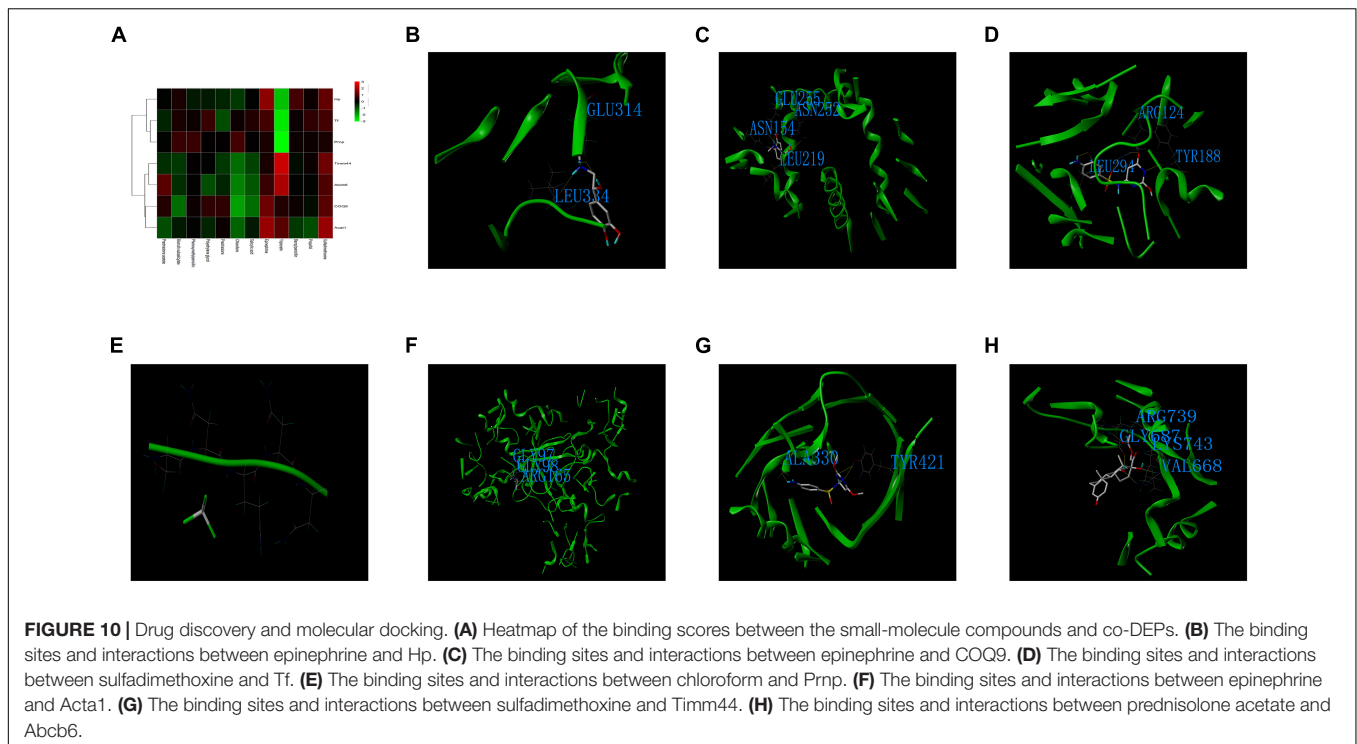


(Figure 10E). Epinephrine was the best match for Acta1, with potential binding at the GLY97, GLY98, and ARG165 residues of Acta1 (Figure 10F). The binding affinity between sulfadimethoxine and Timm44 was the strongest, with potential hydrogen bonding at the ALA330 and TYR421 residues of Timm44 (Figure 10G). Finally, prednisolone acetate was best matched with Abcb6, and ARG739, GLY687, LYS743, and VAL668 of Abcb6 were the potential targets of prednisolone acetate (Figure 10H).

## DISCUSSION

Heart failure with preserved ejection fraction is a complex syndrome that includes many types of clinical phenotypes. Huge pathophysiological differences exist among patients with different clinical HFpEF phenotypes, and no treatment strategy is suitable for all patients with HFpEF (Ge, 2020). Exploring the underlying pathophysiological mechanisms of different types of HFpEF will aid the discovery of personalized therapies and precision medicines for HFpEF treatment. Patients with HFpEF who are also diagnosed with HTN are considered to have vascular-related HFpEF, so exploring the functional connections between HFpEF and HTN will contribute to finding effective therapeutic targets for HFpEF and HTN treatment.

In this study, TMT-labeled quantitative proteomics was used to identify HFpEF- and HTN-related proteins. The functional links between HFpEF and HTN were analyzed at the network, module, and protein levels. Furthermore, molecular docking was used to determine precision medicine targets for HFpEF

and HTN treatment. Seven co-DEPs were found among the HFpEF- and HTN-DEPs identified, including Hp, Tf, COQ9, Acat1, Timm44, Abcb6, and Prnp. Notably, Hp levels are closely related to hypertension and heart failure (Schröcksnadel, 1990; Lu et al., 2019; Rodrigues et al., 2019). Moreover, clinical studies have shown that inflammation plays an important role in the transition from HTN to HFpEF (Quaye, 2008), and that Hp is an indicator of inflammation in cardiovascular diseases (Szelényi et al., 2015). This suggests that Hp could be used to diagnose HTN and HFpEF and that Hp could be an effective therapeutic target for HTN and HFpEF. COQ9 is involved in the basic functions of mitochondria (Ferko et al., 2015), and the impairment of mitochondrial function is a common pathophysiological mechanism underlying both HTN and HFpEF (He et al., 2019; Zeng and Chen, 2019). Thus, COQ9 is also a potential biomarker for HTN and HFpEF. Several studies have shown that the expression of Tf and Prnp is altered in many cardiovascular diseases and that Tf and Prnp may be novel biomarkers for HTN and HFpEF (Gao et al., 2013; Rahim et al., 2018; Roura et al., 2018; Pang et al., 2020). Acta1 is involved in the pathological progression of myocardial remodeling (Pagano et al., 2017; Cañes et al., 2020), which is closely related to the prognosis of HTN and HFpEF (Fortuño et al., 2001; Georgiopolou et al., 2010; Heinzl et al., 2015). Abcb6 and Timm44 are involved in mitochondrial functions and are potential biomarkers for HTN and HFpEF (Boswell-Casteel et al., 2017; Gao et al., 2020). Analysis using the CTD database indicated that there were strong connections between the co-DEPs and cardiovascular diseases in humans, including HF and HTN. Additionally, HFpEF was the most common type of HF, suggesting that

the co-DEPs may be effective therapeutic targets for HFpEF and HTN treatment.

Fever and anemia were found to be important co-DEP-related MM symptoms, which is consistent with previous findings (Bocchi et al., 2013; Tanimura et al., 2015; Burns et al., 2018). The common biological processes of HFpEF and HTN were closely related to energy metabolism. Previous studies have also indicated that mitochondrial oxidative capacity plays an important role in both HFpEF and HTN (Gueugneau et al., 2016; De Jong and Lopaschuk, 2017).

Heart failure with preserved ejection fraction and HTN shared eight overlapping modules, and the main biological functions enriched in these modules were myocardial contraction, energy metabolism, apoptosis, oxidative stress, immune response, and cardiac hypertrophy. We also found that post-translational modification and regulation of actin filaments could play an important role in HFpEF and HTN. Previous research has shown that phosphorylation of cardiac myosin-binding protein-C influences the progress of cross-bridge detachment and that deficient phosphorylation leads to diastolic dysfunction (Rosas et al., 2015). Furthermore, fibroblasts with abnormal proliferation contribute to the progression of HTN to HFpEF (Oatmen et al., 2020). Further research into the biological process of barbed-end actin filament capping may provide new insights.

The study also suggested that chloroform, epinephrine, sulfadimethoxine, and prednisolone acetate could be effective drugs for treating HTN and HFpEF. In addition, epinephrine, sulfadimethoxine, and prednisolone acetate have been widely used in many clinical diseases, but chloroform was not approved drug for human use. It suggested that chloroform maybe an candidate drugs for HTN-HFpEF. Previous studies have shown that gut microbiota dysfunction is closely related to the development of HTN and HFpEF (Hsu et al., 2020; Pakhomov and Baugh, 2020), and some antibiotics that regulate the gut microbiota have shown beneficial effects against HTN and other heart diseases (Chen et al., 2020; Du et al., 2020; Wu et al., 2020). A previous study showed that sulfadimethoxine could also regulate the gut microbiota (Mourand et al., 2014) and contribute to the normalization of blood pressure. Notably, chloroform injection can decrease the mean blood pressure (Loyke, 1971). Furthermore, prednisolone can prevent post-transplantation hypertension in rat renal allograft recipients (de Keijzer et al., 1987), indicating that prednisolone may be an effective drug for treating HTN and HFpEF. For patients with mild essential hypertension, intravenous infusion of small amounts of epinephrine has shown beneficial effects on hemodynamics, renal electrolyte excretion, and blood platelets (Kjeldsen et al., 1988). This indicates that epinephrine may be an effective drug for treating HTN and HFpEF. Most treatment strategies for HFpEF are empiric and are greatly influenced by expert consensus. In addition, some treatment strategies showed beneficial effects in patients with HFpEF, including the use of diuretics to control hypervolemia, treatment with mineralocorticoid antagonists, exercise therapies, and classical treatments for comorbidities. The results of this study, which

are based on molecular docking and bioinformatics analyses, indicated that chloroform, epinephrine, sulfadimethoxine, and prednisolone acetate could be effective medicines for HTN and HFpEF. These drugs could be used to treat HTN and HFpEF, to reduce the occurrence of HFpEF in patients with HTN, or as personalized medicines for patients with HFpEF. Further animal experiments and small-scale clinical trials are needed to elucidate the functions and effects of these drugs in HTN and HFpEF. Nevertheless, it is important to note that chloroform is currently not approved for human use.

According to the enrichment results of the overlapping modules, myocardial contraction was the most important biological function shared between HFpEF and HTN. HTN influences the structure and function of the heart, suppresses myocardial contractions, and increases the prevalence of HFpEF (Chirinos et al., 2017). Previous studies have also noted the importance of myocardial contraction, as impaired diastolic function is a common phenotype of HFpEF and HTN. Here, the co-DEPs *Acat1*, *Tf*, and *Hp* were associated with myocardial contraction. *Acta1* is involved in skeletal muscle thin filament assembly, which influences the contractile force of the heart (Winter et al., 2016). *Tf* and *Hp* are related to the response to lead ion, and result in myocardial contraction-related neurotoxic effects (Pappas et al., 2015). Previous studies have indicated that epinephrine treatment enhances myocardial contraction, but the effects of sulfadimethoxine on myocardial contraction remain unclear (Paur et al., 2012).

Here, we found that energy metabolism is closely related to HFpEF and HTN. These findings are consistent with earlier observations (Baltatu et al., 2017; De Jong and Lopaschuk, 2017). *Acta1*, *Timm44*, and *Abcb6* are involved in fatty acid beta-oxidation and in the biological functions of energy metabolism. In animal experiments, fatty acid beta-oxidation is associated with the severity of myocardial fibrosis. Additionally, it is associated with a risk for HFpEF. Epinephrine, sulfadimethoxine, and prednisolone also have beneficial effects on energy metabolism (Park et al., 2001; Laskewitz et al., 2010; Wang et al., 2019).

Furthermore, apoptosis was found to be an important biological function in HTN and HFpEF. Activation of apoptosis can lead to cardiac dysfunction (Ekhterae et al., 1999), and inhibition of apoptosis can improve heart function and lead to beneficial effects in HFpEF and HTN therapies (Liu et al., 2018; Chen et al., 2019). *Hp* and *Tf* were involved in the response to hypoxia, which promotes cardiomyocyte apoptosis. Previous studies have indicated that *Prnp* is associated with the negative regulation of apoptosis in other diseases (Gao et al., 2019). As chloroform was best matched with *Hp*, *Tf*, and *Prnp*, further studies exploring the anti-apoptotic effect of chloroform in HFpEF and HTN treatment are needed.

In our study, oxidative stress was important in both HFpEF and HTN. Myocardial fibrosis, the major factor leading to myocardial remodeling, was found to be a

common pathological mechanism among HFpEF and HTN. Previous studies using an animal model of HFpEF and HTN have confirmed that the regulation of oxidative stress contributes to the inhibition of myocardial fibrosis (Wu et al., 2016; van der Pol et al., 2018). Similarly, other studies showed that Hp and COQ9 are involved in oxidative stress, including cellular oxidant detoxification and negative regulation of oxidoreductase activity (Swain et al., 2020; Yoshida et al., 2020). However, the effect of epinephrine on oxidoreductase activity in HFpEF and HTN still needs to be explored.

Immune responses are activated in both HFpEF and HTN (Carnevale and Wenzel, 2018; Michels da Silva et al., 2019). Although a treatment strategy targeting the immune response achieved some positive results in HTN, no obvious beneficial effects were observed in HFpEF (Michels da Silva et al., 2019; Zhao et al., 2019). Previous studies have shown that aging influences the immune response in HFpEF and HTN, and here, we found that Hp was associated with aging (De la Fuente et al., 2005; Forman and Goodpaster, 2018). Furthermore, Prnp was associated with the negative regulation of the T cell receptor signaling pathway, which is known to influence the immune response (Wong et al., 2017). Thus, chloroform may be an effective drug for targeting the immune response in HFpEF and HTN treatment.

The results showed that cardiac hypertrophy, which is associated with diastolic function, was significantly associated with HFpEF and HTN (Schmieder, 1990). Angiotensin II receptor blockers (ARBs) have been used in clinical trials for the treatment of HTN, as they not only reduce blood pressure but also have beneficial effects on cardiac hypertrophy, diastolic function, and renal function (Israili, 2000). ARBs also affect the blood pressure of patients with HFpEF, but do not have significant effects on echocardiographic parameters, 6-min walk test distances, or brain natriuretic peptide levels (Parthasarathy et al., 2009). Previous studies have shown that epinephrine can also suppress cardiac hypertrophy. Further research is necessary to determine whether chloroform and prednisolone can induce similar beneficial effects in HFpEF and HTN.

## CONCLUSION

Seven co-DEPs were observed between the HFpEF-DEPs and HTN-DEPs, including Hp, Tf, COQ9, Acat1, Timm44, Abcb6, and Prnp. These co-DEPs were closely related to the main functional similarities of HFpEF and HTN, including myocardial contraction, energy metabolism, apoptosis, oxidative stress, immune response, and cardiac hypertrophy. These co-DEPs may serve as biomarkers and drug targets for HFpEF and HTN. Furthermore, epinephrine, sulfadimethoxine, chloroform, and prednisolone acetate may serve as precision medicines for the treatment of HTN and HFpEF. Our study provides several targets for the development of

personalized therapies and precision medicines to treat HFpEF and other comorbidities.

## LIMITATIONS

There are some limitations to this study. Proteins with low expression levels or those showing insignificant changes could have been ignored in the analyses. Furthermore, these results need to be validated through fundamental research and clinical trials. Further animal experiments will help to explore the function of these drugs in HTN and HFpEF, and small-scale clinical trials will contribute to identifying whether these drugs have similar effects in patients with HTN and those with HFpEF.

## DATA AVAILABILITY STATEMENT

The datasets presented in this study can be found in online repositories. The names of the repository/repositories and accession number(s) can be found in the article/**Supplementary Material**.

## ETHICS STATEMENT

The animal study was reviewed and approved by the Animal Ethics Committee of Shandong University of Traditional Chinese Medicine.

## AUTHOR CONTRIBUTIONS

GZ, JC, and CW conceived the study, acquired the data, and wrote the manuscript. PJ designed the experiments and interpreted the data. YW and YZ performed the experiments and statistical analysis. YJ and XL designed the study and revised the manuscript. All authors read and approved the final manuscript.

## FUNDING

This work has been supported by the National Natural Science Foundation of China (No. 81673970) and the Construction Project of National TCM Clinical Research Base for Hypertension [Guo Zhong Yi Yao Fa (2008) No. 23].

## SUPPLEMENTARY MATERIAL

The Supplementary Material for this article can be found online at: <https://www.frontiersin.org/articles/10.3389/fphys.2021.607089/full#supplementary-material>

## REFERENCES

- Baltatu, O. C., Amaral, F. G., Campos, L. A., and Cipolla-Neto, J. (2017). Melatonin, mitochondria and hypertension. *Cell. Mol. Life Sci.* 74, 3955–3964. doi: 10.1007/s00018-017-2613-y
- Bocchi, E. A., Arias, A., Verdejo, H., Diez, M., Gómez, E., and Castro, P. (2013). The reality of heart failure in Latin America. *J. Am. Coll. Cardiol.* 62, 949–958. doi: 10.1016/j.jacc.2013.06.013
- Borlaug, B. A. (2020). Evaluation and management of heart failure with preserved ejection fraction. *Nat. Rev. Cardiol.* 17, 559–573. doi: 10.1038/s41569-020-0363-2
- Boswell-Casteel, R. C., Fukuda, Y., and Schuetz, J. D. (2017). ABCB6, an ABC Transporter Impacting Drug Response and Disease. *Aaps J.* 20:8. doi: 10.1208/s12248-017-0165-6
- Burns, J. A., Sanchez, C., Beussink, L., Daruwalla, V., Freed, B. H., Selvaraj, S., et al. (2018). Lack of Association Between Anemia and Intrinsic Left Ventricular Diastolic Function or Cardiac Mechanics in Heart Failure With Preserved Ejection Fraction. *Am. J. Cardiol.* 122, 1359–1365. doi: 10.1016/j.amjcard.2018.06.045
- Cañes, L., Martí-Pàmies, I., Ballester-Servera, C., Herraiz-Martínez, A., Alonso, J., Galán, M., et al. (2020). Neuron-derived orphan receptor-1 modulates cardiac gene expression and exacerbates angiotensin II-induced cardiac hypertrophy. *Clin. Sci.* 134, 359–377. doi: 10.1042/cs20191014
- Carnevale, D., and Wenzel, P. (2018). Mechanical stretch on endothelial cells interconnects innate and adaptive immune response in hypertension. *Cardiovasc. Res.* 114, 1432–1434. doi: 10.1093/cvr/cvy148
- Chen, Y. P., Sivalingam, K., Shibu, M. A., Peramaiyan, R., Day, C. H., Shen, C. Y., et al. (2019). Protective effect of Fisetin against angiotensin II-induced apoptosis by activation of IGF-IR-PI3K-Akt signaling in H9c2 cells and spontaneous hypertension rats. *Phytomedicine* 57, 1–8. doi: 10.1016/j.phymed.2018.09.179
- Chen, Y., Zhu, Y., Wu, C., Lu, A., Deng, M., Yu, H., et al. (2020). Gut dysbiosis contributes to high fructose-induced salt-sensitive hypertension in Sprague-Dawley rats. *Nutrition* 7:110766. doi: 10.1016/j.nut.2020.110766
- Chirinos, J. A., Phan, T. S., Syed, A. A., Hashmath, Z., Oldland, H. G., Koppula, M. R., et al. (2017). Late Systolic Myocardial Loading Is Associated With Left Atrial Dysfunction in Hypertension. *Circ. Cardiovasc. Imaging* 10:e006023. doi: 10.1161/circimaging.116.006023
- Cho, J. H., Zhang, R., Kilfoil, P. J., Gallet, R., de Couto, G., Bresee, C., et al. (2017). Delayed Repolarization Underlies Ventricular Arrhythmias in Rats With Heart Failure and Preserved Ejection Fraction. *Circulation* 136, 2037–2050. doi: 10.1161/circulationaha.117.028202
- De Jong, K. A., and Lopuschuk, G. D. (2017). Complex Energy Metabolic Changes in Heart Failure With Preserved Ejection Fraction and Heart Failure With Reduced Ejection Fraction. *Can. J. Cardiol.* 33, 860–871. doi: 10.1016/j.cjca.2017.03.009
- de Keijzer, M. H., Provoost, A. P., Van Aken, M., Wolff, E. D., and Molenaar, J. C. (1987). Prednisolone and posttransplantation hypertension in rat renal allograft recipients. *Transplantation* 43, 353–357. doi: 10.1097/00007890-198703000-00007
- De la Fuente, M., Hernanz, A., and Vallejo, M. C. (2005). The immune system in the oxidative stress conditions of aging and hypertension: favorable effects of antioxidants and physical exercise. *Antioxid. Redox. Signal.* 7, 1356–1366. doi: 10.1089/ars.2005.7.1356
- Dean, J. L., Zhao, Q. J., Lambert, J. C., Hawkins, B. S., Thomas, R. S., and Wesselkamper, S. C. (2017). Editor's Highlight: application of Gene Set Enrichment Analysis for Identification of Chemically Induced, Biologically Relevant Transcriptomic Networks and Potential Utilization in Human Health Risk Assessment. *Toxicol. Sci.* 157, 85–99. doi: 10.1093/toxsci/kfx021
- Drazner, M. H. (2011). The progression of hypertensive heart disease. *Circulation* 123, 327–334. doi: 10.1161/circulationaha.108.845792
- Du, Z., Wang, J., Lu, Y., Ma, X., Wen, R., Lin, J., et al. (2020). The cardiac protection of Baoyuan decoction via gut-heart axis metabolic pathway. *Phytomedicine* 79:153322. doi: 10.1016/j.phymed.2020.153322
- Dunlay, S. M., Roger, V. L., and Redfield, M. M. (2017). Epidemiology of heart failure with preserved ejection fraction. *Nat. Rev. Cardiol.* 14, 591–602. doi: 10.1038/nrcardio.2017.65
- Ekhterae, D., Lin, Z., Lundberg, M. S., Crow, M. T., Brosius, F. C. III, and Núñez, G. (1999). ARC inhibits cytochrome c release from mitochondria and protects against hypoxia-induced apoptosis in heart-derived H9c2 cells. *Circ. Res.* 85, e70–77. doi: 10.1161/01.res.85.12.e70
- Ferko, M., Kancirová, I., Jašová, M., Waczulíková, I., Ěarnická, S., Kucharská, J., et al. (2015). Participation of heart mitochondria in myocardial protection against ischemia/reperfusion injury: benefit effects of short-term adaptation processes. *Physiol. Res.* 64, S617–S625. doi: 10.33549/physiolres.933218
- Forman, D. E., and Goodpaster, B. H. (2018). Weighty Matters in HFpEF and Aging. *JACC Heart Fail.* 6, 650–652. doi: 10.1016/j.jchf.2018.06.016
- Fortuño, M. A., Ravassa, S., Fortuño, A., Zalba, G., and Diez, J. (2001). Cardiomyocyte apoptotic cell death in arterial hypertension: mechanisms and potential management. *Hypertension* 38, 1406–1412. doi: 10.1161/hy1201.099615
- Gao, G., Xuan, C., Yang, Q., Liu, X. C., Liu, Z. G., and He, G. W. (2013). Identification of altered plasma proteins by proteomic study in valvular heart diseases and the potential clinical significance. *PLoS One* 8:e72111. doi: 10.1371/journal.pone.0072111
- Gao, L. P., Xiao, K., Wu, Y. Z., Chen, D. D., Yang, X. H., Shi, Q., et al. (2020). Enhanced Mitophagy Activity in Prion-Infected Cultured Cells and Prion-Infected Experimental Mice via a Pink1/Parkin-Dependent Mitophagy Pathway. *ACS Chem. Neurosci.* 11, 814–829. doi: 10.1021/acscchemneuro.0c00039
- Gao, Z., Peng, M., Chen, L., Yang, X., Li, H., Shi, R., et al. (2019). Prion Protein Protects Cancer Cells against Endoplasmic Reticulum Stress Induced Apoptosis. *Viral. Sin.* 34, 222–234. doi: 10.1007/s12250-019-00107-2
- Gazewood, J. D., and Turner, P. L. (2017). Heart Failure with Preserved Ejection Fraction: diagnosis and Management. *Am. Fam. Phys.* 96, 582–588.
- Ge, J. (2020). Coding proposal on phenotyping heart failure with preserved ejection fraction: a practical tool for facilitating etiology-oriented therapy. *Cardiol. J.* 27, 97–98. doi: 10.5603/cj.2020.0023
- Georgiopoulou, V. V., Kalogeropoulos, A. P., Raggi, P., and Butler, J. (2010). Prevention, diagnosis, and treatment of hypertensive heart disease. *Cardiol. Clin.* 28, 675–691. doi: 10.1016/j.ccl.2010.07.005
- Graziani, F., Varone, F., Crea, F., and Richeldi, L. (2018). Treating heart failure with preserved ejection fraction: learning from pulmonary fibrosis. *Eur. J. Heart Fail.* 20, 1385–1391. doi: 10.1002/ejhf.1286
- Gueugneau, M., Coudy-Gandilhon, C., Meunier, B., Combaret, L., Taillandier, D., Polge, C., et al. (2016). Lower skeletal muscle capillarization in hypertensive elderly men. *Exp. Gerontol.* 76, 80–88. doi: 10.1016/j.exger.2016.01.013
- He, J., Liu, X., Su, C., Wu, F., Sun, J., Zhang, J., et al. (2019). Inhibition of Mitochondrial Oxidative Damage Improves Reendothelialization Capacity of Endothelial Progenitor Cells via SIRT3 (Sirtuin 3)-Enhanced SOD2 (Superoxide Dismutase 2) Deacetylation in Hypertension. *Arterioscler. Thromb. Vasc. Biol.* 39, 1682–1698. doi: 10.1161/atvbaha.119.312613
- Heinzel, F. R., Hohendanner, F., Jin, G., Sedej, S., and Edelman, F. (2015). Myocardial hypertrophy and its role in heart failure with preserved ejection fraction. *J. Appl. Physiol.* 119, 1233–1242. doi: 10.1152/jappphysiol.00374.2015
- Hicklin, H. E., Gilbert, O. N., Ye, F., Brooks, J. E., and Upadhyay, B. (2020). Hypertension as a Road to Treatment of Heart Failure with Preserved Ejection Fraction. *Curr. Hypertens Rep.* 22:82. doi: 10.1007/s11906-020-01093-7
- Hsu, C. N., Yang, H. W., Hou, C. Y., Chang-Chien, G. P., Lin, S., Tan, Y. L., et al. (2020). Maternal Adenine-Induced Chronic Kidney Disease Programs Hypertension in Adult Male Rat Offspring: implications of Nitric Oxide and Gut Microbiome Derived Metabolites. *Int. J. Mol. Sci.* 21:7237. doi: 10.3390/ijms21197237
- Israili, Z. H. (2000). Clinical pharmacokinetics of angiotensin II (AT1) receptor blockers in hypertension. *J. Hum. Hypertens* 14, S73–S86. doi: 10.1038/sj.jhh.1000991
- Kjeldsen, S. E., Os, I., Westheim, A., Lande, K., Gjesdal, K., Hjermann, I., et al. (1988). Hyper-responsiveness to low-dose epinephrine infusion in mild essential hypertension. *J. Hypertens Suppl.* 6, S581–S583. doi: 10.1097/00004872-198812040-00182
- Kjeldsen, S. E., von Lueder, T. G., Smiseth, O. A., Wachtell, K., Mistry, N., Westheim, A. S., et al. (2020). Medical Therapies for Heart Failure With Preserved Ejection Fraction. *Hypertension* 75, 23–32. doi: 10.1161/hypertensionaha.119.14057
- Laskewitz, A. J., van Dijk, T. H., Bloks, V. W., Reijngoud, D. J., van Lierop, M. J., Dokter, W. H., et al. (2010). Chronic prednisolone treatment reduces

- hepatic insulin sensitivity while perturbing the fed-to-fasting transition in mice. *Endocrinology* 151, 2171–2178. doi: 10.1210/en.2009-1374
- Le, D. H., and Pham, V. H. (2017). HGPEC: a Cytoscape app for prediction of novel disease-gene and disease-disease associations and evidence collection based on a random walk on heterogeneous network. *BMC Syst. Biol.* 11:61. doi: 10.1186/s12918-017-0437-x
- Liu, Q., Zhang, Y., Wang, P., Liu, J., Li, B., Yu, Y., et al. (2019). Deciphering the scalene association among type-2 diabetes mellitus, prostate cancer, and chronic myeloid leukemia via enrichment analysis of disease-gene network. *Cancer Med.* 8, 2268–2277. doi: 10.1002/cam4.1845
- Liu, Y., Li, L. N., Guo, S., Zhao, X. Y., Liu, Y. Z., Liang, C., et al. (2018). Melatonin improves cardiac function in a mouse model of heart failure with preserved ejection fraction. *Redox Biol.* 18, 211–221. doi: 10.1016/j.redox.2018.07.007
- Loyke, H. F. (1971). The effect of injected chloroform on renal hypertension. *Anesth. Analg.* 50, 825–828. doi: 10.1213/00000539-197150050-00025
- Lu, D. Y., Lin, C. P., Wu, C. H., Cheng, T. M., and Pan, J. P. (2019). Plasma haptoglobin level can augment NT-proBNP to predict poor outcome in patients with severe acute decompensated heart failure. *J. Invest. Med.* 67, 20–27. doi: 10.1136/jim-2018-000710
- Maitiabola, G., Tian, F., Sun, H., Zhang, L., Gao, X., Xue, B., et al. (2020). Proteome Characteristics of Liver Tissue from Patients with Parenteral Nutrition-Associated Liver Disease. *Nutr. Metab.* 17:43. doi: 10.1186/s12986-020-00453-z
- Messerli, F. H., Rimoldi, S. F., and Bangalore, S. (2017). The Transition From Hypertension to Heart Failure: contemporary Update. *JACC Heart Fail.* 5, 543–551. doi: 10.1016/j.jchf.2017.04.012
- Michels da Silva, D., Langer, H., and Graf, T. (2019). Inflammatory and Molecular Pathways in Heart Failure-Ischemia, HFpEF and Transthyretin Cardiac Amyloidosis. *Int. J. Mol. Sci.* 20:2322. doi: 10.3390/ijms20092322
- Mourand, G., Jouy, E., Bougeard, S., Dheilly, A., Kérouanton, A., Zeitouni, S., et al. (2014). Experimental study of the impact of antimicrobial treatments on *Campylobacter*, *Enterococcus* and PCR-capillary electrophoresis single-strand conformation polymorphism profiles of the gut microbiota of chickens. *J. Med. Microbiol.* 63, 1552–1560. doi: 10.1099/jmm.0.074476-0
- Nwabu, C. C., and Vasan, R. S. (2020). Pathophysiology of Hypertensive Heart Disease: beyond Left Ventricular Hypertrophy. *Curr. Hypertens Rep.* 22:11. doi: 10.1007/s11906-020-1017-9
- Oatmen, K. E., Cull, E., and Spinale, F. G. (2020). Heart failure as interstitial cancer: emergence of a malignant fibroblast phenotype. *Nat. Rev. Cardiol.* 17, 523–531. doi: 10.1038/s41569-019-0286-y
- Pagano, F., Angelini, F., Castaldo, C., Picchio, V., Messina, E., Sciarretta, S., et al. (2017). Normal versus Pathological Cardiac Fibroblast-Derived Extracellular Matrix Differentially Modulates Cardiosphere-Derived Cell Paracrine Properties and Commitment. *Stem Cell. Int.* 2017:7396462. doi: 10.1155/2017/7396462
- Pakhomov, N., and Baugh, J. A. (2020). The Role of Diet-Derived Short Chain Fatty Acids in Regulating Cardiac Pressure Overload. *Am. J. Physiol. Heart Circ. Physiol.* 320, H475–H486. doi: 10.1152/ajpheart.00573.2020
- Pang, B., Hu, C., Wu, G., Zhang, Y., and Lin, G. (2020). Identification of Target Genes in Hypertension and Left Ventricular Remodeling. *Medicine* 99:e21195. doi: 10.1097/md.00000000000021195
- Pappas, C. T., Mayfield, R. M., Henderson, C., Jampilpour, N., Cover, C., Hernandez, Z., et al. (2015). Knockout of *Lmod2* results in shorter thin filaments followed by dilated cardiomyopathy and juvenile lethality. *Proc. Natl. Acad. Sci. U. S. A.* 112, 13573–13578. doi: 10.1073/pnas.1508273112
- Park, W. S., Chang, Y. S., Chung, S. H., Seo, D. W., Hong, S. H., and Lee, M. (2001). Effect of hypothermia on bilirubin-induced alterations in brain cell membrane function and energy metabolism in newborn piglets. *Brain Res.* 922, 276–281. doi: 10.1016/s0006-8993(01)03186-9
- Parthasarathy, H. K., Pieske, B., Weisskopf, M., Andrews, C. D., Brunel, P., Struthers, A. D., et al. (2009). A randomized, double-blind, placebo-controlled study to determine the effects of valsartan on exercise time in patients with symptomatic heart failure with preserved ejection fraction. *Eur. J. Heart Fail.* 11, 980–989. doi: 10.1093/eurjhf/hfp120
- Paulus, W. J., and Tschöpe, C. (2013). A novel paradigm for heart failure with preserved ejection fraction: comorbidities drive myocardial dysfunction and remodeling through coronary microvascular endothelial inflammation. *J. Am. Coll. Cardiol.* 62, 263–271. doi: 10.1016/j.jacc.2013.02.092
- Paur, H., Wright, P. T., Sikkil, M. B., Tranter, M. H., Mansfield, C., O’Gara, P., et al. (2012). High levels of circulating epinephrine trigger apical cardiodepression in a  $\beta$ 2-adrenergic receptor/Gi-dependent manner: a new model of Takotsubo cardiomyopathy. *Circulation* 126, 697–706. doi: 10.1161/circulationaha.112.111591
- Pieske, B., Tschöpe, C., de Boer, R. A., Fraser, A. G., Anker, S. D., Donal, E., et al. (2019). How to diagnose heart failure with preserved ejection fraction: the HFA-PEFF diagnostic algorithm: a consensus recommendation from the Heart Failure Association (HFA) of the European Society of Cardiology (ESC). *Eur. Heart J.* 40, 3297–3317. doi: 10.1093/eurheartj/ehz641
- Quaye, I. K. (2008). Haptoglobin, inflammation and disease. *Trans. R. Soc. Trop. Med. Hyg.* 102, 735–742. doi: 10.1016/j.trstmh.2008.04.010
- Rahim, M. A. A., Rahim, Z. H. A., Ahmad, W. A. W., Bakri, M. M., Ismail, M. D., and Hashim, O. H. (2018). Inverse changes in plasma tetranectin and titin levels in patients with type 2 diabetes mellitus: a potential predictor of acute myocardial infarction? *Acta Pharmacol. Sin.* 39, 1197–1207. doi: 10.1038/aps.2017.141
- Redfield, M. M. (2016). Heart Failure with Preserved Ejection Fraction. *N. Engl. J. Med.* 375, 1868–1877. doi: 10.1056/NEJMc1511175
- Rodrigues, K. F., Pietrani, N. T., Carvalho, L. M. L., Bosco, A. A., Sandrim, V. C., Ferreira, C. N., et al. (2019). Haptoglobin levels are influenced by Hp1-Hp2 polymorphism, obesity, inflammation, and hypertension in type 2 diabetes mellitus. *Endocrinol. Diabetes Nutr.* 66, 99–107. doi: 10.1016/j.endinu.2018.07.008
- Rosas, P. C., Liu, Y., Abdalla, M. I., Thomas, C. M., Kidwell, D. T., Dusio, G. F., et al. (2015). Phosphorylation of cardiac Myosin-binding protein-C is a critical mediator of diastolic function. *Circ. Heart Fail.* 8, 582–594. doi: 10.1161/circheartfailure.114.001550
- Roura, S., Gámez-Valero, A., Lupón, J., Gálvez-Montón, C., Borrás, F. E., and Bayes-Genis, A. (2018). Proteomic signature of circulating extracellular vesicles in dilated cardiomyopathy. *Lab. Invest.* 98, 1291–1299. doi: 10.1038/s41374-018-0044-5
- Schmieder, R. E. (1990). Risk reduction following regression of cardiac hypertrophy. *Clin Exp Hypertens A* 12, 903–916. doi: 10.3109/10641969009073508
- Schröcksnadel, H. (1990). Haptoglobin and free haemoglobin in pregnancy-induced hypertension. *Lancet* 336:1594. doi: 10.1016/0140-6736(90)93383-z
- Swain, N., Samanta, L., Agarwal, A., Kumar, S., Dixit, A., Gopalan, B., et al. (2020). Aberrant Upregulation of Compensatory Redox Molecular Machines May Contribute to Sperm Dysfunction in Infertile Men with Unilateral Varicocele: a Proteomic Insight. *Antioxid. Redox. Signal.* 32, 504–521. doi: 10.1089/ars.2019.7828
- Szelényi, Z., Fazakas, Á., Szénási, G., Kiss, M., Tegze, N., Fekete, B. C., et al. (2015). Inflammation and oxidative stress caused by nitric oxide synthase uncoupling might lead to left ventricular diastolic and systolic dysfunction in patients with hypertension. *J. Geriatr. Cardiol.* 12, 1–10. doi: 10.11909/j.issn.1671-5411.2015.01.001
- Tadic, M., Cuspidi, C., Frydas, A., and Grassi, G. (2018). The role of arterial hypertension in development heart failure with preserved ejection fraction: just a risk factor or something more? *Heart Fail. Rev.* 23, 631–639. doi: 10.1007/s10741-018-9698-8
- Tan, Y., Zuo, W., Huang, L., Zhou, B., Liang, H., Zheng, S., et al. (2020). Nervilifordin F alleviates intestinal ischemia/reperfusion-induced acute lung injury via inhibiting inflammasome and mTOR pathway. *Int. Immunopharmacol.* 89:107014. doi: 10.1016/j.intimp.2020.107014
- Tanimura, M., Dohi, K., Matsuda, M., Sato, Y., Sugiura, E., Kumagai, N., et al. (2015). Renal resistive index as an indicator of the presence and severity of anemia and its future development in patients with hypertension. *BMC Nephrol.* 16:45. doi: 10.1186/s12882-015-0040-6
- van der Pol, A., Gil, A., Tromp, J., Silljé, H. H. W., van Veldhuisen, D. J., Voors, A. A., et al. (2018). OPLAH ablation leads to accumulation of 5-oxoproline, oxidative stress, fibrosis, and elevated fillings pressures: a murine model for heart failure with a preserved ejection fraction. *Cardiovasc. Res.* 114, 1871–1882. doi: 10.1093/cvr/cvy187

- Wang, Q., Wang, C., Wang, B., Shen, Q., Qiu, L., Zou, S., et al. (2019). Identification of RyR2-PBmice and the effects of transposon insertional mutagenesis of the RyR2 gene on cardiac function in mice. *PeerJ*. 7:e6942. doi: 10.7717/peerj.6942
- Winter, J. M., Joureau, B., Lee, E. J., Kiss, B., Yuen, M., Gupta, V. A., et al. (2016). Mutation-specific effects on thin filament length in thin filament myopathy. *Ann. Neurol.* 79, 959–969. doi: 10.1002/ana.24654
- Wong, G. K., Heather, J. M., Barmettler, S., and Cobbold, M. (2017). Immune dysregulation in immunodeficiency disorders: the role of T-cell receptor sequencing. *J. Autoimmun.* 80, 1–9. doi: 10.1016/j.jaut.2017.04.002
- Wu, H., Chen, L., Xie, J., Li, R., Li, G. N., Chen, Q. H., et al. (2016). Periostin expression induced by oxidative stress contributes to myocardial fibrosis in a rat model of high salt-induced hypertension. *Mol. Med. Rep.* 14, 776–782. doi: 10.3892/mmr.2016.5308
- Wu, Q., Xu, Z., Song, S., Zhang, H., Zhang, W., Liu, L., et al. (2020). Gut microbiota modulates stress-induced hypertension through the HPA axis. *Brain Res. Bull.* 162, 49–58. doi: 10.1016/j.brainresbull.2020.05.014
- Yan, F., Gao, M., Gong, Y., Zhang, L., Ai, N., Zhang, J., et al. (2020). Proteomic analysis of underlying apoptosis mechanisms of human retinal pigment epithelial ARPE-19 cells in response to mechanical stretch. *J. Cell. Physiol.* 235, 7604–7619. doi: 10.1002/jcp.29670
- Yoshida, S., Kurajoh, M., Fukumoto, S., Murase, T., Nakamura, T., Yoshida, H., et al. (2020). Association of plasma xanthine oxidoreductase activity with blood pressure affected by oxidative stress level: medCity21 health examination registry. *Sci. Rep.* 10:4437. doi: 10.1038/s41598-020-61463-8
- Yuan, Y., Zhang, Y., Zhang, X., Yu, Y., Li, B., Wang, P., et al. (2016). Deciphering the genetic and modular connections between coronary heart disease, idiopathic pulmonary arterial hypertension and pulmonary heart disease. *Mol. Med. Rep.* 14, 661–670. doi: 10.3892/mmr.2016.5298
- Zeng, H., and Chen, J. X. (2019). Sirtuin 3, Endothelial Metabolic Reprogramming, and Heart Failure With Preserved Ejection Fraction. *J. Cardiovasc. Pharmacol.* 74, 315–323. doi: 10.1097/fjc.0000000000000719
- Zhang, Y., Kong, P., Chen, Y., Yu, Y., Liu, J., Yang, L., et al. (2014). Significant overlapping modules and biological processes between stroke and coronary heart disease. *CNS Neurol. Disord. Drug Targets* 13, 652–660. doi: 10.2174/1871527312666131223115112
- Zhao, T. V., Li, Y., Liu, X., Xia, S., Shi, P., Li, L., et al. (2019). ATP release drives heightened immune responses associated with hypertension. *Sci. Immunol.* 4:eaa6426. doi: 10.1126/sciimmunol.aau6426
- Conflict of Interest:** The authors declare that the research was conducted in the absence of any commercial or financial relationships that could be construed as a potential conflict of interest.
- Publisher's Note:** All claims expressed in this article are solely those of the authors and do not necessarily represent those of their affiliated organizations, or those of the publisher, the editors and the reviewers. Any product that may be evaluated in this article, or claim that may be made by its manufacturer, is not guaranteed or endorsed by the publisher.
- Copyright © 2021 Zhou, Chen, Wu, Jiang, Wang, Zhang, Jiang and Li. This is an open-access article distributed under the terms of the Creative Commons Attribution License (CC BY). The use, distribution or reproduction in other forums is permitted, provided the original author(s) and the copyright owner(s) are credited and that the original publication in this journal is cited, in accordance with accepted academic practice. No use, distribution or reproduction is permitted which does not comply with these terms.